A&A 406, 193–201 (2003)
DOI: 10.1051/0004-6361:20030686

Astronomy & Astrophysics

SV Cam spot activity in February 2001 – March 2002⋆

M. Zboril[1,⋆⋆] and G. Djurašević[2]

[1] Astrophysikalisches Institut, Potsdam, An der Sternwarte 16, 14482, Germany
[2] Astronomical Observatory, Volgina 7, 11160 Belgrade, Yugoslavia and Isaac Newton Institute of Chile, Yugoslav branch

Received 8 November 2002 / Accepted 14 April 2003

Abstract. We present the analysis of new *BVR* light curves for the active star SV Cam. The Roche model with spotted areas on the hotter primary component fits satisfactorily all filter observations yielding two spots in intermediate latitudes and covering about 1.5% each of the stellar surface. Both are ~1000 K cooler than surrounding photosphere. The comparison with an earlier season (January/February 2000) suggests that the spots probably evolved in area longitude and latitude but basic and preferred orientation from previous season is confirmed.

Key words. stars: binaries: eclipsing

1. Introduction

The active star SV Cam (HD44982, p ~ 0.59d, sp. ~ F8, m_V = 9.34) is an eclipsing binary and has been extensively studied since its discovery (Guthnick 1929) due to its asymmetry and overall shape of the light curves and magnetic activity on probably both components. For example Hilditch et al. (1979) gave some arguments in favour of the secondary being responsible for the distortion of light curves. Later on, Cellino et al. (1985) claimed that the hotter primary was an active and spotted component. Özeren et al. (2001) found an excess emission in hydrogen lines connected with the secondary, cooler component of the system and processes like surface plages and prominences. The spectral type of the component stars were derived as G2-3V and K4 by Hilditch et al. (1979) and Pojmański (1996) estimated a new mass ratio, 0.56, and he derived spectral types F5V and K0V from stellar masses for the components.

Among the most recent studies, Albayrak et al. (2001) presented the light and period study of the system and suggested the parameters of the third body orbit. Considering the recent and oldest observations, Zboril (2002) and Lehmann et al. (2002) support a third body. The latter, as well as Kjurkchieva et al. (2002) present also parameters of the components (radii, masses) and hydrogen alpha observations. Kjurkchieva et al. (2002) suggest three possible sources of activity: photospheric spots on the primary, chromospheric-like emission on the secondary and additional emission from circumstellar gas. Lehmann et al. (2002) and Kjurkchieva et al. (2002) offer slightly different mass ratios for the components. Given the spectral type and light curve solutions it is generally agreed that the secondary contributes less than 10% of the light.

The spot properties are of great interest in general and in the case of fast rotators in particular. Since there is a difference in magnetic activity between the Sun and active stars, there may be a considerable difference in their field distribution. Present work on magnetic flux tubes suggests higher spot latitudes for rapidly rotating stars, and perhaps the SV Cam system is a good one to investigate spot properties and its overall activity due to bound and therefore fast rotation of the components.

2. Observations

New observation in *UBVR* filters were obtained on 18 nights with two 0.6 m telescopes at the Skalnaté Pleso and Stará Lesná observatories in the season January 2001 – March 2002. The detectors were photometers OPTEC SSP-5, HAMAMATSU R4457 and EMI 9789 Q multipliers. The differential photometry was performed with the sequence 3xS-3xV-3xCH and sky background and all corrected for differential extinction. The comparison stars were SAO 1045 (S, standard) and SAO 1030 (CH, check). The extinction coefficients can be derived directly from the individual night or seasonal coefficients are loaded from the tables. We used seasonal (roughly summer/winter time) coefficients due to their determination from excellent or very good photometric nights and (decisively) to the air-mass coverage. Similarly, the transformation to the international photometric system is based on first-order equations

$$V - v = c_V * (B - V) \quad (1)$$

$$V - R = c_{VR} * (v - r) \quad (2)$$

Send offprint requests to: M. Zboril,
e-mail: mzboril@aip.de

⋆ Data are available only in electronic form at the CDS via anonymous ftp to cdsarc.u-strasbg.fr (130.79.128.5) or via http://cdsweb.u-strasbg.fr/cgi-bin/qcat?J/A+A/406/193

⋆⋆ on leave from Astronomical Institute, Tatranská Lomnica, 059 60, Slovakia.

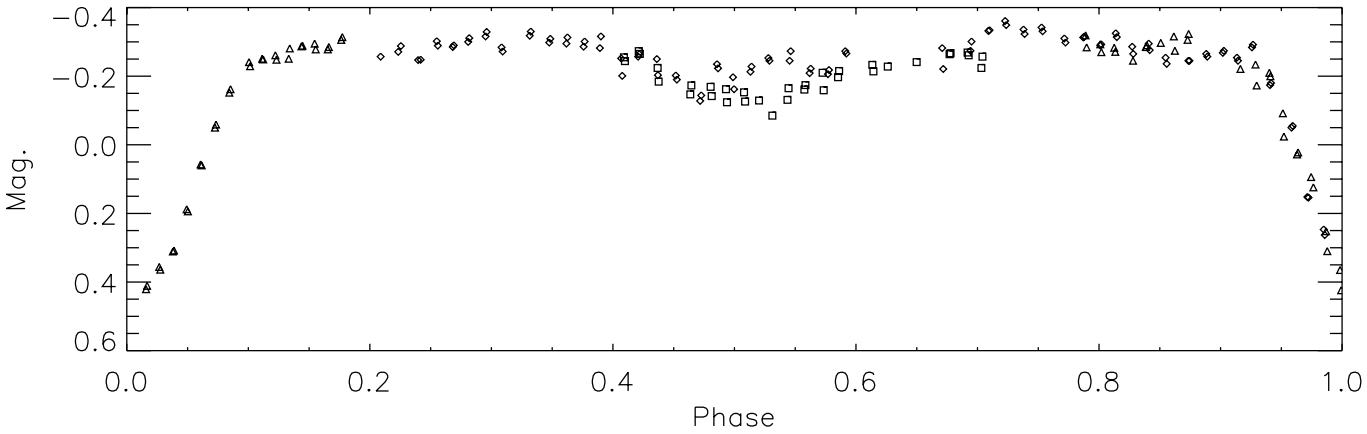

Fig. 1. The original SV Cam **V light curves** in the season 2001. **Diamonds** – night 11.02.2001, **triangles** – night 13.05.2001 and **squares** – night 24.05.2001 respectively.

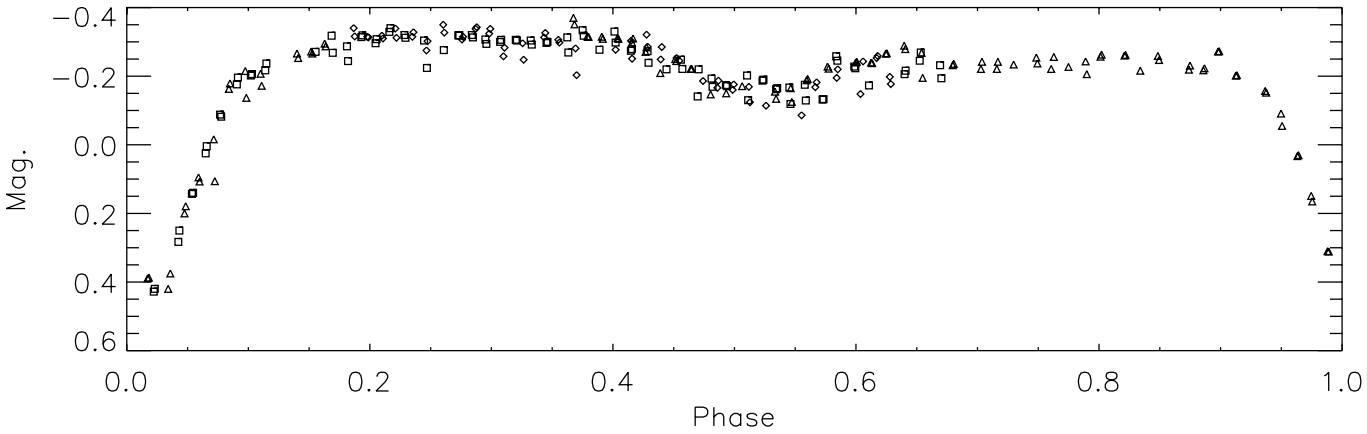

Fig. 2. The original SV Cam **V light curves** in the season 2002. **Diamonds** – night 04.02.2002, **triangles** – night 15.02.2002 and **squares** – night 17.03.2002 respectively.

$$B - V = c_{BV} * (b - v) \tag{3}$$

$$U - B = c_{UB} * (u - b) \tag{4}$$

where the *UBVR* stand for the international system, *ubvr* represent systemic values and $\boldsymbol{c}_{\mathrm{index}}$ the individual filter index coefficient. However, we analysed the data differences in the instrumental system since no attempt is made to involve the observations from different telescopes or to estimate maximal brightness and therefore minimal spot coverage from our data. It is also believed that the transformation to the international system does not reduce the data scatter and errors. Thus, the transformation vectors read

$$(c_{VR}, c_V, c_{BV}, c_{UB})^{SP} = (1.0, -0.08880, 0.98184, 1.11809) \tag{5}$$

$$(c_V, c_{BV}, c_{UB})^{SL} = (-0.08440, 1.11947, 0.98985) \tag{6}$$

for the seasons. The *BVR* light curves were analysed from 10 nights and Table 1 gives the basic log of observations and the differences in instrumental magnitudes in *V* filter between the comparison and check S-CH to demonstrate night stability. We had a precision of about 0.01 mag for the seasons. The values 01 and 02 are codes for nights used in the seasons 2001 and 2002 while *n* means that a different comparison star was observed. These data are in the database but were not included in the analysis. The photometric phases of the light and colour curves were calculated with the following ephemeris (Pojmański 1998):

$$\mathrm{MinI} = \mathrm{HJD}\,2449350.3037 + 0^{\mathrm{d}}.593071 \times E. \tag{7}$$

The observations were sorted for the season 2001 and 2002 respectively and we also constructed mean seasonal light curve 2001-2002 and the merged data were subsequently analysed. Since the secondary minimum of the night 24.05.2001 has the shape of the minima of season 2002, we assigned the data to season 2002.

3. Light curve analysis

To analyze the asymmetric light curves we used the improved version of the Djurašević (1992a) code, which is based on the Roche model and the principles from the paper by Wilson & Devinney (1971). The light-curve analysis was made by applying the inverse-problem method (Djurašević 1992b) based on the modified Marquardt's (1963) algorithm. Optimum model parameters are obtained through the minimization of $S = \Sigma(\mathrm{O}-\mathrm{C})^2$, where O−C is the residual between the observed (LCO) and synthetic (LCC) light curves for a given orbital phase. The minimization of S is done in an iterative cycle

Table 1. Log of observations.

Date	*Filter*	*Obs.*	$S-CH$	*Rem.*
11.02.2001	*BVR*	*SP*	0.290 ± 0.040	01
13.05.2001	*BVR*	*SP*	0.278 ± 0.024	01
14.05.2001	*BV−*	*SL*	0.274 ± 0.013	
24.05.2001	*BVR*	*SP*	0.288 ± 0.023	01
15.10.2001	*BVR*	*SP*	0.280 ± 0.063	
25.10.2001	*BVR*	*SP*	1.143 ± 0.020	*n*
04.02.2002	*BVR*	*SP*	0.294 ± 0.029	02
15.02.2002	*BVR*	*SP*	0.282 ± 0.023	02
09.03.2002	*BV−*	*SL*	2.294 ± 0.014	*n*
17.03.2002	*BVR*	*SP*	0.284 ± 0.033	02

SP-Skalnaté Pleso, SL-Stará Lesná.

of corrections of the model parameters. In this way the inverse-problem method gives us the estimates of system parameters and their standard errors.

The stellar size in the model is described by the filling factors for the critical Roche lobes $F_{1,2}$ of the primary and secondary components which tell us to what degree the stars in the system fill their corresponding critical lobes. For synchronous rotation of the components these factors are expressed as the ratio of the stellar polar radii, $R_{1,2}$, and the corresponding polar radii of the critical Roche lobes, i.e., $F_{1,2} = R_{1,2}/R_{\mathrm{Roche}_{1,2}}$. To achieve more reliable estimates of the model parameters in the light-curve analysis programme, we applied a quite dense coordinate grid, having $72 \times 144 = 10\,368$ individual elementary cells per star. The intensity and angular distribution of the radiation of individual cells are determined by the stellar effective temperature, limb-darkening, gravity-darkening and by the effect of reflection in the system.

In the treatment of the radiation of the components, besides the simple black-body theory and the atmosphere models by Carbon & Gingerich (1969), the current version of the code employs the Basel Stellar Library (BaSeL). We have explored the "corrected" BaSeL model flux distributions, consistent with external empirical calibrations (Lejeune et al. 1997, 1998), and with a large range of effective temperatures $2000\ \mathrm{K} \leq T_{\mathrm{eff}} \leq 35\,000\ \mathrm{K}$, surface gravities, $3 \leq \log g \leq 5$ and metallicity, $-1 \leq [\mathrm{Fe/H}] \leq 1$, where [Fe/H] is the logarithmic metal abundance. The surface gravities can be derived very accurately from the masses and radii of close binary (CB) stars by solving the inverse problem of the light-curve analysis, but the temperature determination is related to the assumed metallicity and strongly depends on the photometric calibration.

In the inverse problem the fluxes are calculated in each iteration for the current values of temperatures and $\log g$ by interpolation both of these quantities in the atmosphere tables, as an input, for a given metallicity of the CB components. The metallicity of the CB components can be different. It is because of this that we can use individual different tables as an input for each star, and in this way choose the best calculations for its particular atmospheric parameters. The two-dimensional flux interpolation in T_{eff} and $\log g$ is based on the application of the *bicubic spline* interpolation (Press et al. 1992). This proved to be a good choice.

By choosing and fixing the particular input switch, the programme for the light-curve analysis can be simply redirected to the Planck or CG approximation, or to the BaSeL model atmospheres. Disagreement between individual *B*, *V*, and *R* solutions decreases if we introduce the "corrected" BaSeL model flux distributions. A change in the assumed metallicity causes a noticable change in the predicted stellar effective temperature. The value of the chemical abundance of the components was obtained by checking several different values around solar metallicity. In the case of SV Cam, the best fit of the *B*, *V*, and *R* light curves was obtained with $[\mathrm{Fe/H}]_{\mathrm{h,c}} = 0.1$ for the metallicity of the components. With this value, the individual *B*, *V*, and *R* solutions are in good agreement. The indices (h,c) refer to the hotter (more-massive) primary and cooler (less-massive) secondary component respectively. The results presented here are given within this stellar atmosphere approximation.

The demonstration of the code for close binary systems is given in Albayrak et al. (2001). Basically the asymmetries in the light curves are assumed to be caused by spots on the system components. The spotted regions are considered as circular spots and characterized by the temperature contrast of the spot against surrounding photosphere, the angular radius, longitude and latitude. Since the stars in the system have external convective envelopes, which can exhibit magnetic activity, we started the "spotted solution" by assuming that the components of SV Cam have cool spots, of the same nature as solar magnetic spots. Moreover, since the results of the light-curve analysis depend on the choice of the adopted working hypothesis, the analysis was carried out within the framework of several hypotheses with spotted areas on the components.

The light curve solution indicates that the primary component is very close to its Roche limit and provides at least 90% of the total light of the system. It is therefore not possible for the cool secondary (which contributes less than 10% to the system light) to be the source of the large distortion in the light curves.

We rejected those hypotheses that produced significantly different values of the parameters for the system and the active spotted areas, estimated by analysing the individual light curves in the *B*, *V*, and *R* passbands. Finally, we chose the Roche model with dark spotted areas on the more massive (hotter) component as the optimum solution. Within this hypothesis the analysis of the light curves yields mutually consistent parameters of the system and active region in the *B*, *V*, and *R* passbands. In this case we obtained a good fit to the observations.

Generally speaking, the estimation of spot latitudes based on the light-curve analysis is somewhat problematic and can lead to incorrect estimates of spot longitudes and radii. Because of that, in the initial phase of the optimization we assume spots to be located in the equatorial zone, and the latitude optimization is included in the final iterations. The numerical tests with artificial light curves have shown that in this way one can estimate the spot parameters with higher accuracy.

The mass-ratio of the components is estimated from spectroscopic observations by several authors. Pojmański (1998) gave the mass ratio of $q = m_{\mathrm{c}}/m_{\mathrm{h}} = 0.56$. In recent analyses we have quite different results. Here, we used two different

values of the mass ratio obtained by Kjurkchieva et al. (2002) and Lehmann et al. (2002) in a radial velocity analysis. These two values are taken as two different hypotheses in the analysis of our light curve.

In the first hypothesis (Hyp. I.) the mass -ratio was fixed to a new revised value of $q = m_c/m_h = 0.593$ by Kjurkchieva et al. (2002) from the radial velocity solution. This estimation is based on spectroscopic material with typical parameters such as $S/N = 120-160$ and a reciprocal linear dispersion of 0.19 Å/pix. Based on this solution, we have $\mathcal{M}_h[M_\odot] \sim 1.47$ for the mass of the primary. To this estimated mass of the primary the appropriate spectral type is F5 V, with effective temperature $T_h = 6440$ K (Lang 1992). This spectral type is in good agreement with the color index $B - V = 0.42$, obtained on the basis of multicolor photometry (Kjurkchieva et al. 2000).

On the other hand, Lehmann et al. (2002) obtained the mass-ratio of the components $q = m_c/m_h = 0.641$ from high-resolution spectroscopic monitoring of SV Cam (resolution 40 000 and $S/N = 150$). Assuming this mass ratio on the basis of the orbital period ($P = 0^d.5930717$), and the semimajor axis ($a_{orb}[\mathcal{R}_\odot] = 3.60$) based on the solution of the radial velocity curve, we have $\mathcal{M}_h[M_\odot] \sim 1.09$ for the mass of the primary. To this estimated mass of the primary the appropriate spectral type is G0 V, with effective temperature $T_h = 6030$ K (Lang 1992). These data made up the second hypothesis in the analysis of our light curve. In both of our hypotheses the temperature of the secondary component is estimated in the inverse problem solving, i.e., it is treated as a free parameter.

Nonlinear limb-darkening laws have been used in the present work to avoid the possible negative influence of the wrong evaulation of limb-darkening coefficients on other parameters in the inverse problem. Following Van Hamme's (1993) paper, whose tables we used, in the programme we chose between the square root approximation for stars hotter than 8000 K and the logarithmic law for stars with lower effective temperatures.

The approximations can be written in the form:

$$I_\lambda(\mu) = I_\lambda(1)(1 - a_\lambda(1 - \mu) - b_\lambda \mu \ln \mu) \quad (8)$$

- logarithmic law

$$I_\lambda(\mu) = I_\lambda(1)(1 - c_\lambda(1 - \mu) - d_\lambda(1 - \sqrt{\mu})) \quad (9)$$

- root square law

where a_λ and b_λ are the logarithmic limb-darkening passband specific coefficients, c_λ and d_λ the root square ones and $\mu = \cos\gamma$. $I_\lambda(1)$ is the passband specific intensity at the center of the stellar disc, and γ is the angle between the line of sight and the emergent flux. The values of the limb-darkening coefficients are derived from the current values of the stellar effective temperature T_{eff} and surface gravity $\log g$ in each iteration, by interpolation for both of these quantities in the Van Hamme (1993) tables. This was achieved by *bicubic spline* or *bi-linear* interpolation (Press et al. 1992).

Following Lucy (1967), Rucinski (1969) and Rafert & Twigg (1980), the gravity-darkening coefficients of the stars, $\beta_{h,c}$, and their albedos, $A_{h,c}$, were set at the values of 0.08 and 0.5, respectively, appropriate for stars with convective envelopes.

We considered that Patkos's (1982) symmetrical reference light curve is very probably clean with respect to spot effects. Since our light curves have a relatively higher noise level and are asymmetric, Patkos' light curve is used in the estimation of initial values of basic system parameters in both hypotheses.

4. Results and discussion

The results of non-linear least-square fitting for both of the hypotheses are presented in Table 2 (Hyp.I. and Hyp.II.). They are obtained from the analysis of observational material for years 2001 and 2002. Because of the noise level and a weak coverage of individual seasonal light curves we believe that this combined material can provide more accurate and reliable estimates of basic system parameters. The initial values of basic system parameters are the data obtained from the analysis of the well- defined Patkos'symmetrical reference light curve. The optimization is done in spot parameters first, and later, in the final phases the basic system parameters are included in the iterative process. Such a procedure gives more realistic estimates of basic system parameters.

The fixed parameters and symbols are properly described in the footnote to the table. Specifically, the spot properties have the following meaning: spot temperature factor $A_S = T_S/T_{star}$, longitude λ_S and latitude ϕ_S. The latitude is measured from stellar equator to north pole (+90°) and south pole (–90°). In order to reduce the number of free parameters in the inverse problem, the temperature contrast of the spot with respect to the surrounding photosphere is fixed to the value $A_S = T_S/T_{star} = 0.84$. This means that the spot temperature is of about 1000 K lower that the temperature of the surrounding photosphere. The ratio 0.84 is a canonical value (e.g. Mullan 1992).

Depending on the hypothesis used (the mass ratio and the temperature of the primary) we have a slight change the basic system parameters, which is expected. However, in both hypotheses we have quite similar results of the active region parameters, i.e., the basic spot properties are effectively insensitive to the hypothesis of given photometric accuracy.

Using the inverse-problem solutions for individual light curves, Fig. 3 presents the optimum fit of the observed light curves (LCO) by the synthetic ones (LCC). The final residuals (O-C) between the observed and optimum synthetic light curves are also given. Finally, a view of the Roche model of SV Cam obtained with the parameters estimated by analysing light curves is provided in the lower part of the panel.

The comparison with the previous season (January/ February 2000, Albayrak et al. 2001) suggests that total spot coverage changed slightly from about 4% of the stellar surface. The spots are located at lower latitudes.

The errors of the parameter estimates arise from the nonlinear least-squares method, on which the inverse-problem method is based. Our estimate of the accuracy in the determination of these parameters is based on the influence of formal errors arising from the nonlinear method of the light-curve analysis. Having in mind the errors of the input parameters of the model, which are treated as fixed in the inverse-problem method, the real errors of the parameters will definitely be larger (approximately 2–3 times). The main contribution comes

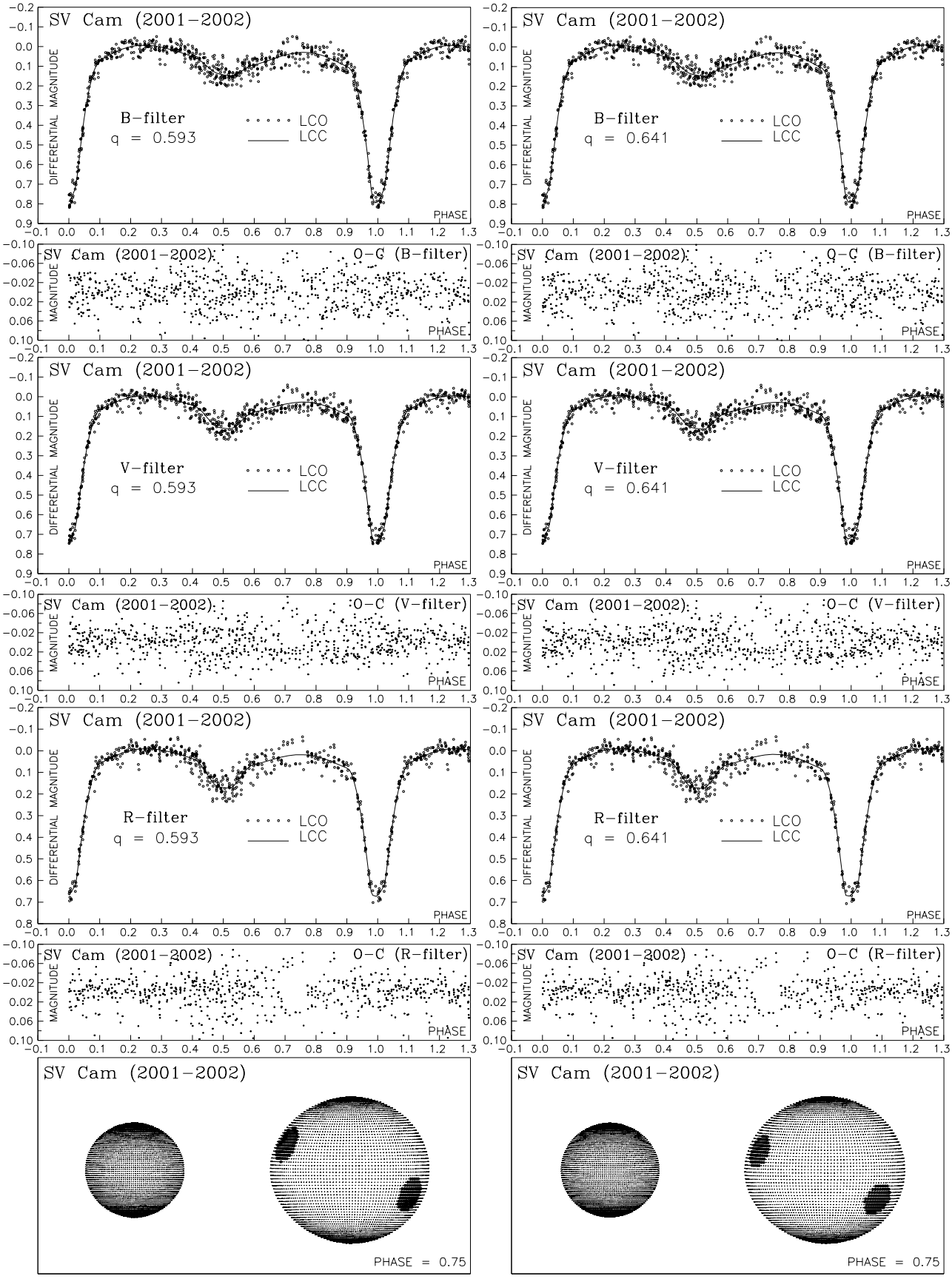

Fig. 3. The observed (LCO) and synthetic (LCC) light curves of the SV Cam system in *BVR* filters respectively. The bottom panel is the Roche model for the system at orbital phase 0.75. Hypotheses Hyp. I. and II. respectively.

Table 2. Results of the analysis of the SV Cam light curves obtained by solving the inverse problem for the Roche model with two active cool areas on the more-massive (hotter) component. (**Hyp. I.**: $q = m_c/m_h = 0.593$, $T_h = 6440$; **Hyp. II.**: $q = m_c/m_h = 0.641$, $T_h = 6030$).

Quantity	B – filter Hyp. I.	V – filter Hyp. I.	R – filter Hyp. I.	B – filter Hyp. II.	V – filter Hyp. II.	R – filter Hyp. II.
n	618	623	511	618	623	511
$\Sigma(O-C)^2$	0.6970	0.5852	0.5157	0.6987	0.5873	0.5167
σ	0.0336	0.0307	0.0318	0.0337	0.0307	0.0318
$q = m_c/m_h$	0.593	0.593	0.593	0.641	0.641	0.641
T_h	6440	6440	6440	6030	6030	6030
θ_{S1}	13.8 ± 0.6	14.0 ± 0.7	14.4 ± 1.0	12.4 ± 0.6	11.8 ± 0.7	13.2 ± 1.0
λ_{S1}	332.0 ± 5.0	333.7 ± 6.9	336.4 ± 6.9	331.3 ± 5.6	331.6 ± 7.0	336.0 ± 6.8
φ_{S1}	20.1 ± 7.4	22.1 ± 8.8	18.7 ± 9.5	13.3 ± 9.2	17.1 ± 10.7	13.7 ± 9.1
θ_{S2}	13.6 ± 0.6	13.9 ± 0.6	14.1 ± 0.8	12.8 ± 0.7	13.1 ± 0.7	13.5 ± 0.9
λ_{S2}	214.2 ± 5.8	214.8 ± 7.0	212.4 ± 7.6	223.4 ± 5.4	227.5 ± 6.9	217.0 ± 7.4
φ_{S2}	−21.1 ± 9.6	−16.7 ± 13.5	−18.8 ± 13.8	−23.0 ± 8.4	−20.0 ± 10.9	−22.7 ± 10.3
T_c	4489 ± 91	4485 ± 73	4473 ± 66	4337 ± 75	4330 ± 60	4282 ± 62
F_h	0.841 ± 0.004	0.845 ± 0.004	0.846 ± 0.005	0.857 ± 0.004	0.864 ± 0.004	0.859 ± 0.005
F_c	0.692 ± 0.003	0.695 ± 0.003	0.694 ± 0.004	0.676 ± 0.003	0.681 ± 0.003	0.678 ± 0.004
i	89.6 ± 1.5	89.3 ± 1.9	89.5 ± 2.9	88.9 ± 1.6	89.3 ± 1.2	88.6 ± 2.2
a_h	0.808	0.715	0.622	0.827	0.742	0.649
b_h	0.232	0.275	0.282	0.185	0.257	0.269
a_c	0.839	0.799	0.732	0.832	0.799	0.742
b_c	−0.156	0.006	0.111	−0.164	0.005	0.114
Ω_h	3.533	3.519	3.517	3.572	3.548	3.565
Ω_c	3.917	3.903	3.910	4.126	4.104	4.116
R_h	0.337	0.338	0.338	0.337	0.340	0.338
R_c	0.217	0.218	0.217	0.216	0.218	0.217
$L_h/(L_h + L_c)$	0.966	0.941	0.921	0.965	0.939	0.920
$\mathcal{M}_h\,[M_\odot]$	1.47 ± 0.06			1.09 ± 0.05		
$\mathcal{M}_c\,[M_\odot]$	0.87 ± 0.06			0.70 ± 0.02		
$\mathcal{R}_h\,[R_\odot]$	1.37 ± 0.03			1.26 ± 0.02		
$\mathcal{R}_c\,[R_\odot]$	0.87 ± 0.03			0.79 ± 0.02		
$\log g_h$	4.33 ± 0.03			4.28 ± 0.03		
$\log g_c$	4.50 ± 0.03			4.49 ± 0.02		
M^h_{bol}	3.63 ± 0.03			4.10 ± 0.03		
M^c_{bol}	6.18 ± 0.05			6.55 ± 0.06		
$a_{orb}\,[R_\odot]$	3.94 ± 0.06			3.60 ± 0.05		

FIXED PARAMETERS:
$[Fe/H]_{h,c} = 0.1$ – accepted metallicity of the components
$q = m_c/m_h$ – mass ratio of the components,
T_h – temperature of the more-massive (hotter) star,
$f_h = f_c = 1.00$ – nonsynchronous rotation coefficients of the components,
$\beta_{h,c} = 0.08$ – gravity-darkening coefficients of the components,
$A_{h,c} = 0.5$ – albedo coefficients of the components.
$A_{S1,2} = T_{S1,2}/T_h = 0.84$ – spots' temperature coefficient,
BaSeL approximation of the stellar atmospheres ($[Fe/H]_{h,c} = 0.1$ – accepted metallicity of the components).

Note: n – number of observations, $\Sigma(O-C)^2$ – final sum of squares of residuals between observed (LCO) and synthetic (LCC) light curves, σ – standard deviation of the observations, $\theta_{S1,2}$, $\lambda_{S1,2}$ and $\varphi_{S1,2}$ − spots' angular dimensions, longitudes and latitudes (in arc degrees), $F_{h,c}$ – filling factors for the critical Roche lobe of the hotter (more-massive) and cooler (less-massive) star, T_c – temperature of the less-massive cooler star, i – orbit inclination (in arc degrees), $a_{h,c}, b_{h,c}$ – nonlinear limb-darkening coefficients of the components in the logarithmic law, $\Omega_{h,c}$ – dimensionless surface potentials of the primary and secondary, $R_{h,c}$ – polar radii of the components in units of the distance between the component centres, $L_h/(L_h + L_c)$ – luminosity of the hotter star (including spots on the cooler one), $\mathcal{M}_{h,c}\,[M_\odot]$ – stellar masses in solar units, $\mathcal{R}_{h,c}\,[R_\odot]$ – mean radii of stars in solar units, $\log g_{h,c}$ – logarithm (base 10) of the mean surface acceleration (effective gravity) for system stars, $M^{h,c}_{bol}$ – absolute bolometric magnitudes of SV Cam components, and $a_{orb}\,[\mathcal{R}_\odot]$ – orbital semi-major axis in units of solar radius.

from the error in effective temperature of the primary fixed on the basis of its spectral type, with a relatively high uncertainty. Thus, the estimated error of the secondary component's temperature is significantly larger than the tabular values obtained under the assumption that the temperature of the primary is accurate. The errors in the estimates of the stellar radii are included (through the filling factors), while the errors in the masses are not formally used (the mass ratio is treated as fixed), but certainly they contribute to the errors of the system parameter estimation. Because of these, the real error bars in the parameter estimates might be larger than the values given in the tables.

Having in mind the shape of the total light curve at secondary minimum and maximum (see Fig. 1) it appears that the location of active regions changed during the analysed time. Thus, a further step in our analysis is to separate the seasonal light curves and to estimate the spot parameters from their analysis. Taking into account the light curves with good coverage of orbital phases we separate the seasonal light curves for the years 2001 and 2002. We analysed them only for spot parameters while the basic system parameters obtained from the entire observational material were taken from Table 2. Over such a short period one cannot expect the change of basic system parameters, and they can be more reliably estimated from the combined observational material. The estimated seasonal spot parameters are given in Table 3. Since the differences in the fitting quality and estimated spot parameters for both hypotheses are very similar, we give only the results obtained within the Hyp. I. The graphical presentation of the results is given in Fig. 4.

It is evident from Table 3 and Fig. 4 that the Roche model with cool spot areas on the hotter primary component gives a satisfactory fit to the analysed light curves. The seasonal changes in the light curves can be explained by the change in location and size of spots.

Table 3. Seasonal (2001 and 2002) spot parameters of the SV Cam, obtained by light-curve analysis with system parameters given in Table 2 (Hyp. I.).

2001			
Quantity	B – filter	V – filter	R – filter
n	150	155	151
$\Sigma(O-C)^2$	0.1260	0.1278	0.0988
σ	0.0291	0.0288	0.0257
θ_{S1}	13.7 ± 0.7	13.0 ± 1.0	14.2 ± 1.0
λ_{S1}	329.2 ± 8.0	323.0 ± 11.1	335.5 ± 8.9
φ_{S1}	6.4 ± 28.2	10.7 ± 16.2	13.9 ± 14.5
θ_{S2}	18.0 ± 0.9	18.7 ± 1.1	19.2 ± 1.1
λ_{S2}	88.1 ± 10.8	102.6 ± 11.9	101.7 ± 11.4
φ_{S2}	−51.7 ± 5.9	−49.9 ± 5.9	−48.3 ± 6.1
2002			
Quantity	B – filter	V – filter	R – filter
n	367	364	362
$\Sigma(O-C)^2$	0.3532	0.2760	0.3269
σ	0.0311	0.0276	0.0301
θ_{S1}	16.7 ± 0.9	16.2 ± 1.1	17.8 ± 1.2
λ_{S1}	288.9 ± 5.7	284.2 ± 6.4	282.2 ± 6.7
φ_{S1}	25.9 ± 10.0	22.4 ± 14.6	24.9 ± 14.5
θ_{S2}	12.5 ± 0.6	12.8 ± 0.7	13.1 ± 0.8
λ_{S2}	206.2 ± 6.8	211.0 ± 7.5	203.9 ± 9.3
φ_{S2}	−11.2 ± 16.7	−12.4 ± 18.9	−13.7 ± 19.2

Note: n – number of observations, $\Sigma(O-C)^2$ – final sum of squares of residuals between observed (LCO) and synthetic (LCC) light curves, σ – standard deviation of the observations, $\theta_{S1,2}$, $\lambda_{S1,2}$ and $\varphi_{S1,2}$ – spots' angular dimensions, longitudes and latitudes (in arc degrees).

5. Conclusions

We present a research note on *BVR* light curve analysis from the season February 2001 to March 2002 and a comparison is made with the previous season (January/February 2000). The model with cool spots on hotter (larger) component of the system fits satisfactorily all filter light curves. The basic spot properties are the following:

1. two spots on the hot component each covering 1.5% of the stellar surface as a minimum spot coverage;
2. the spots are at intermediate latitudes, about 20° and –20° respectively (all merged dataset) and one spot is orientated towards the secondary and the second spot is on the opposite side;
3. the spots temperature is 1000 K cooler than the surrounding photosphere;
4. if the spots are identical to the previous season (2000), the spots have evolved in area, longitude and latitude but certain directions are maintained (orientation towards the secondary and the opposite side location for second spot).

It is probable that the system is more densely spotted but the light curves allow us to determine only the signatures producing significant contrast. This however seems to be enough to inter-compare the spot configuration of the previous season.
Magnetically induced solar activity includes diverse phenomena as well as time-dependent effects such as spots. All these processes have stellar counterparts, often on a dramatically enhanced scale. It is generally believed that cool spots on stars can be used to trace magnetic flux that emerges from an *unknown* dynamo process in the stellar interior. Flux-tube models predict higher spot latitudes with higher rotational angular velocity but with larger depth of convective envelope as well. It is also believed that the SV Cam system with its rotational period is a good candidate to test recent flux-tube models and processes associated with. Notwithstanding, practically all active phenomena have been observed not only on RS CVn stars but systems like BY Dra stars, T Tauri objects, FK Com stars etc. In many systems, however, the spot distribution is not stable over more than few rotational cycles (e.g. Rice & Strassmeier 2000).

Acknowledgements. The work was supported by the grant No. 2/1024/21 of Slovak Grant Agency for Science, and by the Ministry for Sciences and Technology of Serbia through the project 1191 "Stellar physics". MZ also acknowledges gratefully the support from AIP Potsdam (DFG grant STR 645/1).

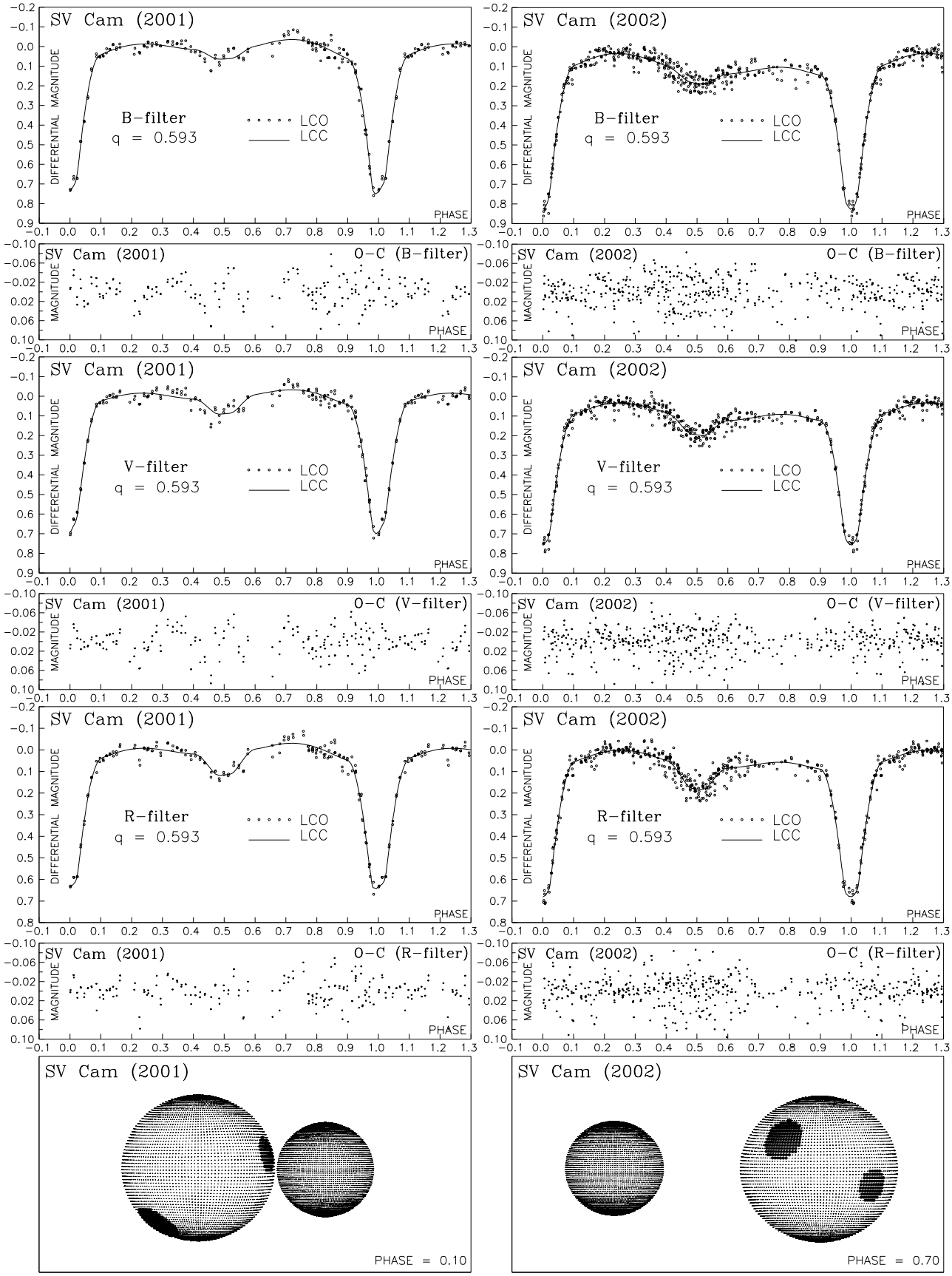

Fig. 4. Observed (LCO) and final synthetic (LCC) light curves of the SV Cam with final O–C residuals obtained by analysing *B*, *V* and *R* observations (2001 – left, 2002 – right) and the view of the systems at orbital phase 0.10 (2001) and 0.7 (2002) obtained with the parameters estimated by analysing observations.

References

Albayrak, B., Demircan, O., Djurašević, G., Erkapić, S., & Ak, H. 2001, A&A, 376, 158

Carbon, D., & Gingerich, O. 1969, in Theory and Observation of Normal Stellar Atmospheres, ed. O. Gingerich (Cambridge: MIT Press), 377

Cellino, A., Scaltriti, F., & Busso, M. 1985, A&A, 144, 315

Djurašević, G. 1992a, Ap&SS, 196, 241

Djurašević, G. 1992b, Ap&SS, 197, 17

Guthnick, P. 1929, Astron. Nachr., 235, 83

Hilditch, R. W., Harland, D. M., & McLean, B. J. 1979, MNRAS, 187, 797

Kjurkchieva, D., Marchev, D., & Ogloza, W. 2000, Acta Astron., 50, 517

Kjurkchieva, D. P., Marchev, D. V., & Zola, S. 2002, A&A, 386, 548

Lang, K. R. 1992, Astrophysical Data: Planets and Stars (New York Inc.: Springer-Verlag)

Lehmann, H., Hempelmann, A., & Wolter, U. 2002, A&A, 392, 963

Lejeune, T., Cuisinier, F., & Buser, R. 1997, A&AS, 125, 229

Lejeune, T., Cuisinier, F., & Buser R. 1998, A&AS, 130, 65

Lucy, L. B. 1967, Zs. f. Ap., 65, 89

Marquardt D. W. 1963, J. Soc. Ind. Appl. Math., 11, No. 2, 431

Mullan, D. J. 1992, in Surface Inhomogeneities on Late-Type Stars, ed. P. B. Byrne, & D. J. Mullan, Lecture Notes in Physics, 397, 233

Özeren, F. F., Gunn, A. G., Doyle, J. G., & Jevremovič, D. 2001, A&A, 366, 202

Patkos, L. 1982, Comm. Konkoly Obs., 80, 1

Pojmański, G. 1998, Acta. Astron., 48, 711

Press, W. H, Teukolsky, S. A, Vetterling, W. T., & Flannery, B. P. 1992, Numerical Recipes in Fortran, The Art of Scientific Computing, Second Edition (New York: Cambridge University Press), 120

Rafert, J. B., & Twigg, L. W. 1980, MNRAS, 139, 78

Rice, J., & Strassmeier, K. G. 2000, A&AS, 147, 151

Rucinski, S. M. 1969, Acta Astr., 19, 245

Van Hamme, W. 1993, AJ, 106, 2096

Wilson, R. E., & Devinney, E. J. 1971, ApJ, 166, 605

Zboril, M. 2002, IBVS, No. 5303